J. Biochem. 123, 839-846 (1998)

# Effects of Point Mutations at the Flexible Loop Alanine-145 of *Escherichia coli* Dihydrofolate Reductase on Its Stability and Function[1]

**Eiji Ohmae,* Kenji Ishimura,* Masahiro Iwakura,† and Kunihiko Gekko*,[2]**

*Department of Materials Science and Graduate Department of Gene Science, Faculty of Science, Hiroshima University, Kagamiyama, Higashi-Hiroshima, Hiroshima 739-8526; and †Joint Research Center for Atom Technology (JRCAT), National Institute of Bioscience and Human-Technology, 1-1 Higashi, Tsukuba, Ibaraki 305-8566

Received for publication, October 27, 1997

**To elucidate the role of a flexible loop (residues 142-149) in the stability and function of *Escherichia coli* dihydrofolate reductase, alanine-145 in this loop was substituted by site-directed mutagenesis with ten amino acids (Glu, Phe, Gly, His, Ile, Leu, Arg, Ser, Thr, and Val). The amount of three mutant proteins (A145E, A145I, and A145L) in cells was too small to allow the measurement of circular dichroism (CD) spectra and urea unfolding. The CD spectra of other seven mutants were identical with those of the wild-type DHFR, indicating that the native conformation of DHFR was not affected by the mutations. The free energy change of unfolding by urea decreased with an increase in the hydrophobicity of amino acid residues introduced, A145T > A145R > A145G ≧ A145S ≧ A145H > A145V > wild-type ≧ A145F. The steady-state kinetic parameters for the enzyme reaction, $K_m$ and $k_{cat}$, were only slightly influenced by the mutations. These results suggest that site 145 in the flexible loop plays an important role in the stability but has little or no effect on the native structure and function of this enzyme. The characteristics of the mutations are discussed in comparison with those of mutations at site 67 [Ohmae *et al.* (1996) *J. Biochem.* 119, 703-710] and at site 121 [Gekko *et al.* (1994) *J. Biochem.* 116, 34-41] in two other flexible loops.**

**Key words: dihydrofolate reductase, enzyme function, point mutation, role of flexible loop, structural stability.**

Dihydrofolate reductase (DHFR) [EC 1.5.1.3] from *Escherichia coli* is a monomeric protein of 159 amino acids with no disulfide bond or prosthetic group. The three-dimensional structure of the enzyme in the crystalline state was determined for the binary DHFR-methotrexate complex (*1*) and for the apoenzyme (*2*). The structure and properties of the enzyme in solution have been extensively studied by many approaches: equilibrium and kinetic unfolding-refolding analyses (*3-5*), NMR spectroscopy (*6, 7*), and enzyme kinetics (*8-10*). However, the conformation and function of DHFR have remained largely mysterious. For example, there seem to be at least two conformers with different affinities for cofactor, substrate, and inhibitor (*6-8, 10*). It is very rarely the case that the Gly95-Gly96 linkage has a *cis*-conformation. Such conformers may be necessary for the flexibility of the structure to accommodate the cofactor, NADPH, and the substrate, dihydrofolate ($H_2F$), since the protein is small.

To address the structure-function relationships of this enzyme, many mutation studies have been performed involving amino acid substitutions at more than 25 positions. However, most of them were related to positions surrounding the active site, and only a limited number concerned amino acid substitution in the flexible loops. DHFR has several flexible loops, such as residues 9-24, 64-72, 117-131, and 142-149, as revealed by the large B-factor of X-ray crystallographic data (*1, 2*) (Fig. 1). The B-factor of these loops largely changes when the enzyme is bound with the inhibitor methotrexate (MTX), suggesting some participation of the loops in the enzymatic function. Recent findings by Sawaya and Kraut demonstrated that these loops move actively and cooperatively on binding NADPH and $H_2F$ (*11*). A matter of concern is how mutations at loop regions affect the stability and function of this enzyme. The answer to this question should provide a new insight into the protein dynamics and catalytic mechanism of this enzyme. In this context, Li *et al.* found that the rate of hydride-transfer from NADPH to $H_2F$ decreases markedly when four residues (Met16-Ala19) in the most mobile loop (residues 9-24) are replaced by a glycine (*12*). Tan *et al.* showed that deletion of two residues (Gly45-Lys46) from a flexible loop of human DHFR decreases the $V_{max}$ value but has almost no effect on the $K_m$ values and pH profile of its enzymatic activity (*13*). In previous studies, we found that site-directed mutagenesis at glycines 67 and

[1] This work was supported by a Grant-in-Aid for Scientific Research from the Ministry of Education, Science, Sports and Culture of Japan (No. 09261225).

[2] To whom correspondence should be addressed.

Abbreviations: CD, circular dichroism; DHFR, dihydrofolate reductase; $H_2F$, dihydrofolate; $H_4F$, tetrahydrofolate; MTX, methotrexate; PAGE, polyacrylamide gel electrophoresis; SDS, sodium dodecyl sulfate.

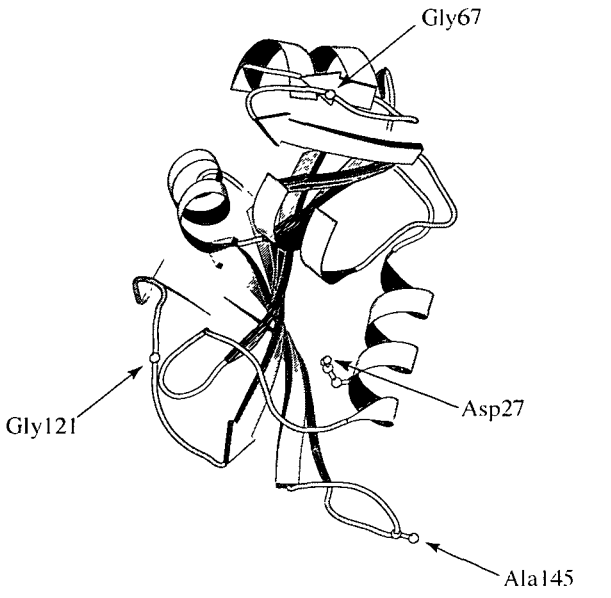


Fig. 1. **The structure of a DHFR-MTX binary complex (B-chain).** Taken from Bolin *et al.* (*1*). Positions of Gly67, Gly121, Ala145, and Asp27, an active site residue, are indicated by arrows. Side chains of Ala145 and Asp27 are shown by the ball-and-stick model. This figure was produced using the graphics program Molscript (*50*).

121 in flexible loops (residues 64-72 and 117-131, respectively) significantly influences the stability and enzyme function, although the $\alpha$-carbons at these sites are respectively 29 and 19 Å distant from the catalytic residue Asp27 (*14-16*). The adiabatic compressibility, which is directly related to the volume fluctuation, is influenced by these mutations, depending on the stability and enzyme activity (*17*). Interestingly, a recent NMR study confirmed that these two sites have the highest order parameter in each loop, namely, they are extremely mobile in solution (*18*). These findings suggest that the flexible loops may be key domains in determining the flexibility, stability, and function of this enzyme.

In the present study, to elucidate the role of another flexible loop (residues 142-149) connecting the $\beta$G and $\beta$H strands, we constructed ten mutants of alanine-145, one of the most mobile residues in this loop. The effects of mutations on the stability and function were discussed in comparison with those of mutations at sites 67 and 121 (*15, 16*). The structural characteristics of this site are as follows. The mobility (B-factor) decreases when the enzyme is bound with MTX, as it does for the loop 117-131, although it increases for the loop 64-72 (*1, 2*). The amino acid side chain at site 145 is exposed to the solvent, although those at sites 67 and 121 are directed toward the interior of the protein molecule. The $\alpha$-carbon at site 145 is only 14 Å distant from the catalytic residue Asp27.

## MATERIALS AND METHODS

*Plasmid and Mutant Constructions*—All mutant DHFR genes were produced with plasmid pTZwt1-3 (3.7 kb) (*19*), which produced 1,400-fold overexpression of the wild-type DHFR protein. The following three oligonucleotides were synthesized and used for site-directed mutagenesis utilizing a three-step PCR reaction: 5′AGCGAATTCCACGATGCTGATNNWCAGAACTCGCATAGCTATTGTTTCGAAATCCTCGAG3′ (A145X-N), where N is a mixture of four bases and W a mixture of A and T; 5′GGGGATCCTTAACGACGCTCGAGGATTTCGAAACAATAGCTATGCGAGTT3′ (WT-BC); and 5′CCCGGATCCGCTCTTGACAATTAGTTAACTATTTG3′ (P35-1). To construct the C-terminal region of the mutant DHFR genes containing site 145, the first PCR reaction was performed using the wild-type DHFR template DNA obtained by *Bam*HI digestion of plasmid pTZwt1-3, primers A145X-N, and WT-BC. In the second PCR, the wild-type DHFR template DNA obtained by *Bam*HI digestion of plasmid pTZwt1-3, P35-1 primer, and products of the first PCR were used to construct the overall mutant genes. Finally, products of the second PCR were subjected to PCR with P35-1 and WT-BC primers for amplifying the mutant genes. The obtained mutant genes were digested by *Bam*HI, cloned into pUC118 (*20*), and sequenced with a Pharmacia ALF DNA sequencer II to determine the amino acid residue at site 145.

*Protein Purification*—The wild-type and mutant DHFR proteins were purified as described previously (*16*). The concentration of the wild-type DHFR was determined using a molar extinction coefficient of 31,100 $M^{-1} \cdot cm^{-1}$ at 280 nm (*8*). The concentrations of mutant DHFRs were determined assuming the same molar extinction coefficient, since the amino acids introduced in this study have no or negligibly small chromophores.

*Circular Dichroism Spectra*—Far-ultraviolet circular dichroism (CD) spectra of the wild-type and mutant DHFRs were measured at 15°C using a Jasco J-720W spectropolarimeter as described previously (*16*). The solvent conditions were 10 mM potassium phosphate (pH 7.0) containing 0.1 mM EDTA and 0.1 mM dithiothreitol. The protein concentration was kept at about 20 $\mu$M. Each spectrum was an average of 16 measurements.

*Equilibrium Unfolding*—Equilibrium unfolding of DHFRs with urea (ultrapure product from Schwarz/Mann) was monitored by means of CD measurements at 222 nm and 15°C with a Jasco J-720W spectropolarimeter as described previously (*16*). The solvent conditions were 10 mM potassium phosphate (pH 7.0) containing 0.1 mM EDTA and 1.4 mM 2-mercaptoethanol. The protein concentration was kept at about 20 $\mu$M. All samples were fully equilibrated at each denaturant concentration before the CD spectra were measured. The observed molar ellipticity data, $[\theta]$ (30-38 points), were directly fitted to the two-state unfolding model, native (N)$\rightleftharpoons$unfolded (U), by means of nonlinear least-squares regression analysis with the SALS program (*21*), as follows

$$[\theta] = \{[\theta]_N + [\theta]_U \exp(-\Delta G_u/RT)\}/\{1+\exp(-\Delta G_u/RT)\} \quad (1)$$

where $\Delta G_u$ is the Gibbs free energy change of unfolding, $R$ the gas constant, $T$ the absolute temperature, and $[\theta]_N$ and $[\theta]_U$ the molar ellipticities of the native and unfolded forms, respectively. $[\theta]_N$ and $[\theta]_U$ at a given urea concentration were estimated by assuming the same linear dependence of ellipticity in the transition region as in the pure native (pre-transition region) and unfolded states (post-transition region). The free energy change of unfolding, $\Delta G_u$, in Eq. 1 was assumed to be linearly dependent on the urea concentration (*22*)

$$\Delta G_u = \Delta G^\circ_u + m[\text{urea}] \quad (2)$$

where $\Delta G^\circ_u$ is the free energy change of unfolding in the absence of a denaturant, and the slope, $m$, is a parameter reflecting the cooperativity of the transition. The urea concentration at the mid-point of the transition ($\Delta G_u = 0$) was defined as $C_m$.

*Steady-State Kinetics*—The steady-state kinetics of the enzyme reaction were studied spectrophotometrically using a Jasco V-520 spectrophotometer at 25°C as described previously (*16*). The concentrations of dihydrofolate, $H_2F$ (Sigma), and NADPH (Oriental Yeast) were determined spectrophotometrically using molar extinction coefficients of 28,000 $M^{-1}\cdot cm^{-1}$ at 282 nm and 6,200 $M^{-1}\cdot cm^{-1}$ at 339 nm, respectively. The enzyme concentrations were determined by the methotrexate titration method (*23*) to eliminate the effects of denatured species which may be produced during storage. The buffer used was 33 mM succinic acid containing 44 mM imidazole and 44 mM diethanolamine, whose pH was adjusted to 7.0 with acetic acid or tetraethylammonium hydroxide. The Michaelis constant ($K_m$) and the rate constant of catalysis ($k_{cat}$) were measured with various concentrations of $H_2F$ (0.3 to 20 $\mu$M) at a saturated concentration of NADPH (60 $\mu$M). The final concentrations of the enzymes were 0.5-1.5 nM. The enzyme solutions were preincubated with NADPH for 10 min to eliminate the hysteresis effect (*24*), and the reaction was started by adding $H_2F$ to the preincubated mixture. The initial velocities ($v$) of the enzyme reaction were calculated from the time course of absorbance at 340 nm using a differential molar extinction coefficient of 11,800 $M^{-1}\cdot cm^{-1}$ (*25*). The $K_m$ and $k_{cat}$ values were determined with the following equation by nonlinear least-squares analysis with the SALS program

$$v = (k_{cat}[E][S])/(K_m + [S]) \quad (3)$$

where [E] is the enzyme concentration, and [S] the initial substrate concentration.

## RESULTS

*Circular Dichroism Spectra*—Figure 2 shows far-ultraviolet CD spectra of the wild-type and four mutant DHFRs (A145G, A145T, A145V, and A145H) at 15°C and pH 7.0. Similar spectra were observed for three other mutant DHFRs (A145R, A145S, and A145F). The spectra of these seven mutants were clearly identical within the limits of experimental error with that of the wild-type DHFR, which has a negative peak of $-8{,}500$ deg·cm²·dmol⁻¹ at 219 nm and a positive peak of 11,200 deg·cm²·dmol⁻¹ at 196 nm (*16*). This suggests that the conformation of these mutants was not affected by the residues at site 145. These results were quite different from those of the mutations at sites 67 and 121, since their CD spectra were clearly affected by the mutations (*14-16*). Since the accumulation of three mutant DHFRs (A145I, A145L, and A145E) in cells was very small, they could not be purified as a single band on SDS-PAGE, and accurate CD measurement was therefore impossible.

*Equilibrium Unfolding*—Figure 3 shows typical plots of the molar ellipticities at 222 nm of the wild-type and four mutant DHFRs as a function of the urea concentration at 15°C. Similar transition curves were observed for three other mutant DHFRs (A145G, A145H, and A145F). The transition curves were obviously shifted from that of wild-type DHFR to higher urea concentration for A145R and to lower urea concentration for A145V. Those for the other five mutants were almost same or slightly shifted to lower urea concentration. These results imply that all mutations at site 145 affected the structural stability of DHFR.

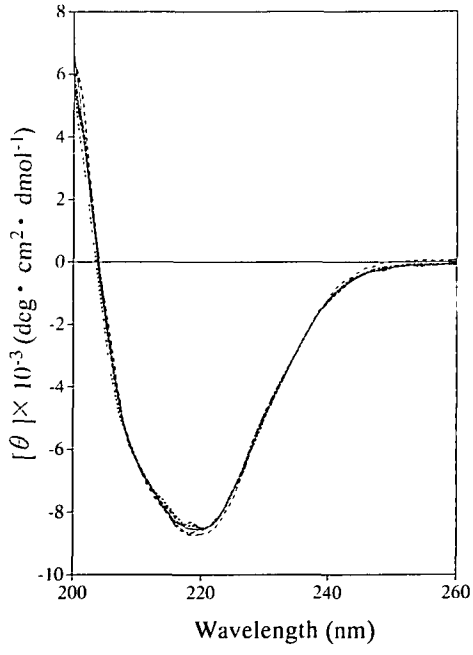


Fig. 2. **Far-ultraviolet circular dichroism spectra of the wild-type and four mutant DHFRs at 15°C and pH 7.0.** The solvent used was 10 mM potassium phosphate (pH 7.0) containing 0.1 mM EDTA and 0.1 mM dithiothreitol. (—) Wild-type DHFR; (·····) A145H; (----) A145G; (----) A145T; (----) A145V.

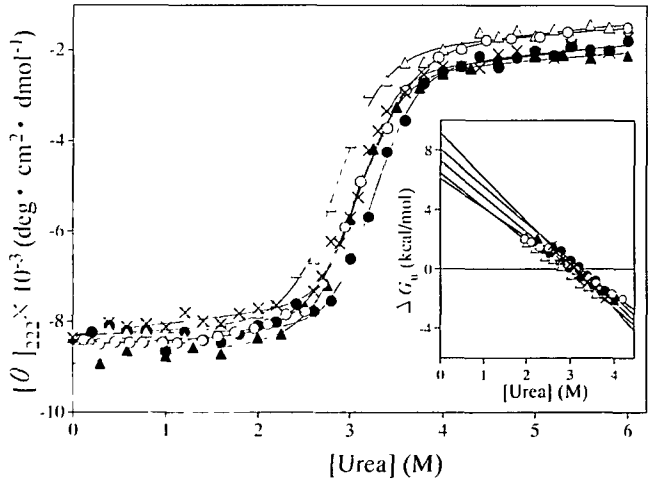


Fig. 3. **Molar ellipticity of the wild-type and four mutant DHFRs at 222 nm as a function of the urea concentration at 15°C.** The solvent used was 10 mM potassium phosphate (pH 7.0) containing 0.1 mM EDTA and 1.4 mM 2-mercaptoethanol. (○) Wild-type DHFR; (●) A145R; (△) A145V; (▲) A145S; (×) A145T. Solid lines represent the theoretical fits to a two-state model with the parameter values shown in Table I (see "MATERIALS AND METHODS"). The inset shows the dependence of $\Delta G_u$ on the urea concentration.

The CD spectra of A145T at various urea concentrations exhibited an isoellipticity point at 210 nm, and the same transition curve was obtained at any wavelength in the range of 200-260 nm (data not shown). This indicates that the unfolding of the mutant DHFRs essentially follows the two-state transition model, as in the case of wild-type and other mutant DHFRs (*3, 26, 27*). The different ellipticities of each mutant in the absence of urea are due to small errors in protein concentrations, but this does not affect the thermodynamic data of the stability. Then, the free energy change of unfolding, $\Delta G_u$, was calculated with Eq. 1 and plotted against the urea concentration in the inset of Fig. 3. The good linear relationship observed allows us to calculate the free energy change of unfolding in water, $\Delta G^\circ_u$, the slope, $m$, and the denaturant concentration at $\Delta G_u = 0$, $C_m$. The results of the calculation are listed in Table I. Evidently, these parameters are dependent on the amino acid introduced: the stability decreased in the order of A145T > A145R > A145G ≧ A145S ≧ A145H > A145V > wild-type ≧ A145F.

The $m$ values of all mutant DHFRs were more negative than that of the wild-type DHFR, indicating the enhanced cooperativity of the transition. The $m$ values changed almost in parallel with $\Delta G^\circ_u$, as revealed by the high

TABLE I. **Thermodynamic parameters for urea denaturation of the wild-type and mutant DHFRs at 15°C.**[a]

| DHFRs | $V$[b] (ml/mol) | $\Delta g^\circ_{tr}$[c] (kcal/mol) | $\Delta G^\circ_u$[d] (kcal/mol) | $m$[d] (kcal/mol·M) | $C_m$[d] (M) |
|---|---|---|---|---|---|
| Wild-type[e] | 52.0 | 0.5 | 6.08±0.18 | −1.96±0.06 | 3.11 |
| A145G | 34.8 | 0.0 | 7.38±0.22 | −2.42±0.07 | 3.05 |
| A145S | 51.9 | −0.3 | 7.28±0.26 | −2.38±0.09 | 3.05 |
| A145T | 68.3 | 0.4 | 9.13±0.26 | −2.95±0.08 | 3.10 |
| A145V | 82.4 | 1.5 | 6.45±0.20 | −2.27±0.07 | 2.85 |
| A145H | 90.3 | 0.5 | 7.25±0.21 | −2.44±0.07 | 2.97 |
| A145F | 112.8 | 2.5 | 5.94±0.17 | −2.01±0.06 | 2.96 |
| A145R | 118.8 | −3.0 | 8.05±0.23 | −2.48±0.07 | 3.26 |

[a]The solvent used was 10 mM potassium phosphate (pH 7.0) containing 0.1 mM EDTA and 1.4 mM 2-mercaptoethanol. [b]Molar volume of amino acids (*49*). [c]The transfer free energy change of introduced amino acid side chains from organic solvent to water (*43*). [d]The parameters $\Delta G^\circ_u$, $m$, and $C_m$ were calculated assuming a linear relationship between $\Delta G_u$ and the urea concentration (Eq. 2). [e]Gekko *et al.* (*15*).

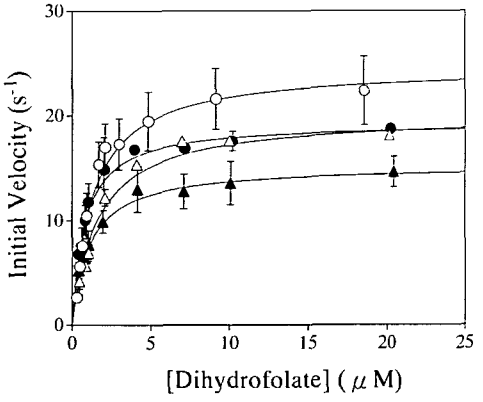


Fig. 4. **Initial velocity of the enzymatic reaction of the wild-type and three mutant DHFRs as a function of the dihydrofolate concentration at 25°C.** The solvent used was 33 mM succinic acid, 44 mM imidazole, and 44 mM diethanolamine (pH 7.0), containing 60 μM NADPH. The concentrations of enzymes were 0.5-1.5 nM. (○) Wild-type DHFR; (●) A145S; (△) A145T; (▲) A145V. Solid lines represent the theoretical fits to Eq. 3 with the parameter values shown in Table II.

TABLE II. **Steady-state kinetic parameters for the enzyme activity of the wild-type and mutant DHFRs at 25°C.**[a]

| DHFRs | $K_m$ (μM) | $k_{cat}$ ($s^{-1}$) | $k_{cat}/K_m$ ($\mu M^{-1} \cdot s^{-1}$) |
|---|---|---|---|
| Wild-type[b] | 1.3±0.1 | 24.6±3.1 | 18.9 |
| A145G | 1.2±0.1 | 21.1±2.4 | 17.6 |
| A145S | 0.8±0.0 | 19.3±0.5 | 24.1 |
| A145T | 1.6±0.1 | 20.0±0.1 | 12.5 |
| A145V | 1.1±0.2 | 15.2±1.5 | 13.8 |
| A145H | 0.7±0.2 | 18.8±0.8 | 26.9 |
| A145F | 1.2±0.3 | 27.6±7.9 | 23.0 |
| A145R | 1.4±0.2 | 19.9±1.5 | 14.2 |
| A145E | 0.8±0.0 | 15.2±1.3 | 19.0 |
| A145L | 1.0±0.0 | 15.1±1.7 | 15.1 |
| A145I | 0.8±0.0 | 13.7±1.1 | 17.1 |

[a]The solvent used was 33 mM succinic acid containing 44 mM imidazole and 44 mM diethanolamine (pH 7.0). [b]Ohmae *et al.* (*16*).

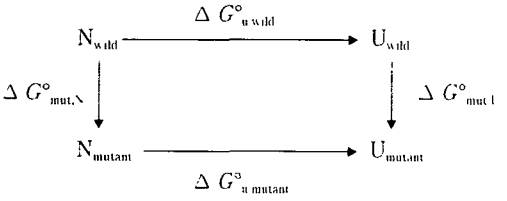


Scheme 1

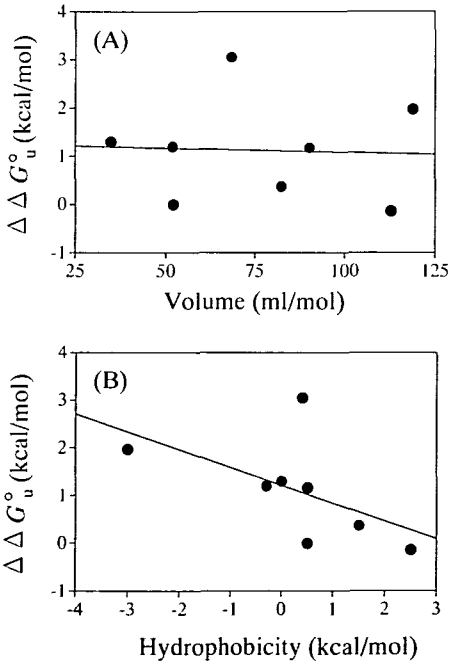


Fig. 5. **Plots of $\Delta\Delta G^\circ_u$ against the molar volume (A) and the hydrophobicity (B) of introduced amino acid side chains for the wild-type and mutant DHFRs at site 145.** The $\Delta\Delta G^\circ_u$ values were calculated with Eq. 5 (see "DISCUSSION"). The molar volume is cited from Zamyatnin (*49*). The hydrophobicity is cited from Nozaki and Tanford (*43*). Solid lines were drawn by the least-squares method with the exception of A145T in panel B.

correlation coefficient between the two parameters ($r$ = 0.967). This was also the case for mutant DHFRs at sites 67 and 121 (*15, 16*). On the other hand, the $C_m$ values of all mutants except A145R were smaller than that of the wild-type DHFR, and there was only low correlation between $C_m$ and $\Delta G^\circ_u$ ($r$=0.514). These results suggest that the structural stability of DHFR was largely affected by the cooperativity of unfolding. A145R is the first case of a single mutant having a larger $C_m$ value than the wild-type DHFR among the 25 single mutants at three flexible loops that we have examined, although this property has been found in two double-mutant DHFRs, G67V/G121A, and G67V/G121Y (*28*).

*Steady-State Kinetics*—Figure 4 shows typical plots of the initial velocity of the enzyme reaction as a function of the substrate concentration ($H_2F$). Similar hyperbolic curves were observed for other mutant DHFRs. The Michaelis constant, $K_m$, and the rate constant of catalysis, $k_{cat}$, were calculated using Eq. 3 and listed in Table II. The $K_m$ and $k_{cat}$ values of the wild-type DHFR were consistent with the data reported by another group (*9*), although the $k_{cat}$ values seemed slightly smaller. The $K_m$ values of the mutant DHFRs varied in the range of 0.8 $\mu$M (A145E and A145I) to 1.6 $\mu$M (A145T), and the $k_{cat}$ values varied in the range of 13.7 $s^{-1}$ (A145I) to 27.6 $s^{-1}$ (A145F). Considering the limits of experimental error, these values are not greatly different from those of the wild-type DHFR. These results are very similar to those for mutations at site 67 (*16*), but greatly different from those for mutations at site 121, which showed a large decrease in $k_{cat}$ and an almost constant $K_m$ value (*15*). Thus the mutations at site 145 did not have so large an effect on the enzyme function of DHFR as those at site 121, even though site 145 is closer (14 Å) to catalytic residue Asp27 than site 121 (19 Å).

## DISCUSSION

As shown in this study, amino acid substitution at site 145 brought about considerably large changes in the stability, but only small or no changes in the enzyme function and secondary structure of DHFR. These results demonstrate the importance of this site as well as sites 67 and 121 for DHFR, although they are located in flexible loops far from the active site. A matter of concern is how such a local change in the primary structure of a flexible loop is coupled to the stability and function of the overall protein structure. This problem will be discussed below on the basis of statistical analyses of the results for mutations at site 145 in comparison with those for mutations at sites 67 and 121 (*15, 16*).

*Structure of Mutant DHFRs*—As shown in Fig. 2, the CD spectra of mutant DHFRs overlapped that of the wild-type DHFR within the limits of experimental error, indicating that the secondary structure of DHFR was not modified by mutations at site 145. This result is interesting, since we found that the CD spectrum of DHFR was generally influenced by mutations at sites 67 and 121 (*15, 16*), and other groups have reported similar findings (*5, 29*). An important characteristic of site 145 different from sites 67 and 121 is the orientation of the side chain: the side chain of Ala145 is exposed to the solvent (Fig. 1), but those of Gly67 and Gly121 are buried in the protein molecule. Computer simulation predicts that, unlike Gly67 and Gly121, Ala145 can be substituted with any other amino acid except threonine without accompanying movements of the backbone polypeptide chain (Segawa, S., personal communication). Therefore, it is probable that mutations at site 145 do not largely disturb the conformation of the protein to modify the CD spectrum, although in the case of Gly67 and Gly121 the conformational change due to overcrowding of the bulky side chain may affect the exciton pair of two aromatic residues, Trp47 and Trp74, leading to modification of the peptide CD (*5*).

*Structural Stability*—As shown in Table I, the free energy change of unfolding in water, $\Delta G^\circ_u$, was markedly influenced by mutations at site 145. Considerably large changes in $\Delta G^\circ_u$ were also observed for mutations at sites 67 and 121 (*15, 16*). A noticeable difference is that most mutants at site 145 have a larger $\Delta G^\circ_u$ value than the wild-type DHFR, while most mutants at sites 67 and 121 have a lower value. In either case, it is of interest that the highly mobile sites located in the flexible loops play an important role in the structural stability of DHFR. Recently, it has been found that an identical substitution, for example, from valine to alanine at the different sites, does not necessarily have the same effects on the structural stability or the enzyme activity of small globular proteins (*30-33*). These results indicate that the position and surrounding structure of the substituted residue are the important factors for the stability and function of proteins. Our results demonstrate that not only the $\alpha$-helices and $\beta$-sheets but also the flexible loops can influence the stability and function of the enzymes.

The mutation effects on the stability can be quantitatively analyzed with the free energy diagram, where N and U are the native and unfolded states, respectively, and $\Delta G^\circ_{mut,N}$ and $\Delta G^\circ_{mut,U}$ denote the free energy changes of mutation (amino acid substitution) in the native and unfolded states, respectively. According to this diagram,

$$\Delta\Delta G^\circ_u = \Delta G^\circ_{u,mutant} - \Delta G^\circ_{u,Wild} = \Delta G^\circ_{mut,U} - \Delta G^\circ_{mut,N} \quad (5)$$

Many experimental data show proportionality between $\Delta\Delta G^\circ_u$ and the hydrophobicity of introduced amino acid side chains (*34-37*), and this is consistent with the consensus that the hydrophobic interaction is the dominant stabilizing force for the native protein structure (*38*). However, some discrepancies have been found with $\lambda$ repressor protein (*39*), staphylococcal nuclease (*29, 30, 40*), and DHFR (*3*). It is known that the protein structure is destabilized by introducing nonpolar residues to a surface amino acid of $\lambda$-*Cro* protein (*41*) and cytochrome *c* (*42*). These results indicate that the effects of mutations are highly site-dependent. It is *a priori* difficult from thermodynamics to determine which of the native and unfolded structures predominantly contributes to the modified stability of mutants, since $\Delta G^\circ_{mut,N}$ and $\Delta G^\circ_{mut,U}$ or the corresponding heat capacity changes are generally unknown. However, the stabilizing mechanism may be partly understood through the correlation of $\Delta\Delta G^\circ_u$ with structural parameters of the amino acid residues introduced.

Figure 5 shows plots of the $\Delta\Delta G^\circ_u$ values, which were calculated from the results in Table I, as a function of the molar volume ($V$) and the hydrophobicity ($\Delta g^\circ_{tr}$) estimated by Nozaki and Tanford (*43*) of introduced amino acid side chains at site 145. As shown in Fig. 5A, there is no correlation between $\Delta\Delta G^\circ_u$ and $V$ (correlation coefficient,

$r=0.051$), suggesting that the bulkiness of the side chains at site 145 is not responsible for stability of the mutants. This is consistent with the side chain at this site being exposed to the solvent. In this context, it is noteworthy that a distinctly negative correlation was found between the two parameters for mutants at site 67 and 121 whose side chains are buried in the protein molecule (*1, 2*). A possible explanation for the latter case is that overcrowding of the bulky side chain at sites 67 and 121 may strain the backbone chain conformation of the native structure, leading to increased flexibility or decreased stability of the overall structure (*15, 16*). A similar overcrowding effect was found for the stability of mutant DHFRs at Val88, the central residue in the hinge region (residues 85-91) (*29*). In fact, there is a considerable body of experimental evidence (NMR, X-ray, and compressibility) showing that the flexibility or rigidity of the native structure is an important determining factor of protein stability (*44-46*). However, the lack of correlation between $\Delta\Delta G^\circ_u$ and $V$ suggests that the effect of mutations at site 145 on the stability could not be explained by such a flexibility-mediated mechanism, which is dominantly ascribed to the native structure.

As shown in Fig. 5B, on the other hand, there is a good correlation between $\Delta\Delta G^\circ_u$ and $\Delta g^\circ_{tr}$ except for A145T ($r=0.864$), indicating that the structure is destabilized with increasing the hydrophobicity of the side chains. A similar but less distinct correlation between these two parameters was also found for mutants at sites 67 and 121 (*15, 16*). A possible explanation for such a reverse hydrophobic effect is that the nonpolar side chains introduced are less exposed to the solvent in the unfolded state than in the native state, since most polar and charged side chains introduced would be exposed to the solvent in both the native and unfolded states. This means that $\Delta G^\circ_{mut,U}$ is smaller than $\Delta G^\circ_{mut,N}$ because of the depressed free energy increase in the unfolded state, leading to the decrease in $\Delta\Delta G^\circ_u$. This may be possible for a mutation at a hyper or highly exposed position, although there is no direct experimental evidence supporting this idea. Pakula and Sauer proposed that this is the case for mutations at the hyperexposed site 26 of $\lambda$-*Cro* protein (*41*). Bowler *et al.* also found that a surface amino acid not hyperexposed has a similar reverse hydrophobic effect on the stability of cytochrome *c* (*42*). Therefore, it may be possible that the reverse hydrophobic effect observed here is mainly caused by the modification of the unfolded state. If this is the case, the question arises of to what extent the nonpolar surface is buried in the unfolded protein molecule relative to the native state. No estimate is presently available, but the slope of $\Delta\Delta G^\circ_u$ *vs.* $\Delta g^\circ_{tr}$ plots may be a measure of this value when the side chains in the native state are assumed to be completely exposed to the solvent, that is, $\Delta G^\circ_{mut,N}=\Delta g^\circ_{tr}$. Thus, we may tentatively predict that at most 40% of the side chains at site 145 would be buried in the protein molecule as a result of the unfolding process.

As shown in Fig. 5B, the $\Delta\Delta G^\circ_u$ value of A145T deviates greatly from the regression line. This is not caused by experimental artifacts, since the value is an average of four individual experiments and the experimental error is sufficiently small. Thus we may expect some special stabilizing mechanism for A145T different from other mutants. One speculation is that the side chain of this mutant may form hydrogen bonds with groups surrounding this position, although detailed understanding of the structure must await X-ray or NMR analyses.

A noticeable characteristic of the mutations at site 145 is that $\Delta G^\circ_u$ increases in proportion to the $m$ value, while it is not dependent on $C_m$ (Table I). Similar results were obtained for the mutants at site 67 ($r=0.795$ and 0.001 for $m$ and $C_m$, respectively) and site 121 ($r=0.72$ and 0.40 for $m$ and $C_m$, respectively) (*15, 16*). Although interpretation of the $m$ value remains controversial (*47, 48*), these results might constitute evidence that the stability of these mutants at the flexible sites is predominantly determined by the modified cooperativity of unfolding. A definite correlation between $\Delta G^\circ_u$ and $m$ was also found for many mutants of staphylococcal nuclease (*30, 31, 40*).

*Enzyme Function*—As shown in Table II, the kinetic parameters of mutant DHFRs at site 145 were not markedly different from those of the wild-type DHFR. Considering the large decrease in the $k_{cat}$ values for site 121 mutants, it is interesting that the enzyme activity was not greatly influenced by mutations at site 145, although this site is nearer to the active site residue, Asp27, than site 121. Bystroff and Kraut suggested, from the X-ray crystal structure, that the Met20 loop (residues 9-24) folds over the binding sites for the pteridine and nicotinamide mononucleotide moieties, and two loops, 117-131 and 142-149, perform supporting roles of this conformational change (*2*). Recently, Sawaya and Kraut showed that the Met20 loop interacts with Asp122 in the "closed" and "open" conformations, and with Ser148 in the "occluded" conformation of the ligand-induced loop movements in a catalytic cycle of DHFR (*11*). As shown by CD spectra in Fig. 2, the mutations at Ala145 did not affect the native structure of DHFR, and thus the Met20 loop could interact with both loops for site 145 mutants as well as the wild-type DHFR, with only little effect on the enzyme activity. As described above, however, Gly121 cannot be substituted with any other amino acid without causing movement of the backbone polypeptide chain, and thus the interaction of Asp122 with the Met20 loop may be disrupted, thereby decreasing the enzymatic activity of DHFR. This presumption may be supported by the fact that the depressed activity of G121L can be recovered by introducing a second mutation at site 122 (the double mutant G121L/D122E) (our unpublished data). An interesting question is whether a mutation at site 145 can also restore the decreased enzymatic activity of the mutant DHFRs at site 121. The double-mutation study at sites 121 and 145 is now in progress in our laboratory.

As demonstrated in this study, site-directed mutagenesis of alanine at site 145, located in a flexible loop (residues 142-149), has a large effect on the stability, but little or no effect on the structure and enzymatic activity of *E. coli* DHFR. The reverse hydrophobic effect on the stability suggests that the main effect of this mutation is modification of the unfolded structure, as was expected from the exposed orientation of the side chain at this site. The minimal effect on the enzymatic activity suggests that the interactions between three loops (residues 9-24, 117-131, and 142-149) in a catalytic cycle of this enzyme are not essentially affected by mutation at site 145.

We wish to thank the Nagoya University Computer Center for the use of the SALS program.

REFERENCES


1. Bolin, J.T., Filman, D.J., Matthews, D.A., Hamlin, R.C., and Kraut, J. (1982) Crystal structures of *Escherichia coli* and *Lactobacillus casei* dihydrofolate reductase refined at 1.7 Å resolution. *J. Biol. Chem.* **257**, 13650-13662
2. Bystroff, C. and Kraut, J. (1991) Crystal structure of unliganded *Escherichia coli* dihydrofolate reductase: Ligand-induced conformational changes and cooperativity in binding. *Biochemistry* **30**, 2227-2239
3. Garvey, E.P. and Matthews, C.R. (1989) Effects of multiple replacements at a single position on the folding and stability of dihydrofolate reductase from *Escherichia coli*. *Biochemistry* **28**, 2083-2093
4. Perry, K.M., Onuffer, J.J., Gittelman, M.S., Barmat, L., and Matthews, C.R. (1989) Long-range electrostatic interactions can influence the folding, stability, and cooperativity of dihydrofolate reductase. *Biochemistry* **28**, 7961-7968
5. Kuwajima, K., Garvey, E.P., Finn, B.E., Matthews, C.R., and Sugai, S. (1991) Transient intermediates in the folding of dihydrofolate reductase as detected by far-ultraviolet circular dichroism spectroscopy. *Biochemistry* **30**, 7693-7703
6. Birdsall, B., Feeney, S.J.B., Tendler, S.J., Hammond, D.J., and Roberts, G.C.K. (1989) Dihydrofolate reductase: Multiple conformations and alternative modes of substrate binding. *Biochemistry* **28**, 2297-2305
7. Falzone, C.J., Wright, P.E., and Benkovic, S.J. (1991) Evidence for two interconverting protein isomers in the methotrexate complex of dihydrofolate reductase from *Escherichia coli*. *Biochemistry* **30**, 2184-2191
8. Fierke, C.A., Johnson, K.A., and Benkovic, S.J. (1987) Construction and evaluation of the kinetic scheme associated with dihydrofolate reductase from *Escherichia coli*. *Biochemistry* **26**, 4085-4092
9. Howell, E.E., Booth, C., Farnum, M., Kraut, J., and Warren, M.S. (1990) A second-site mutation at phenylalanine-137 that increases catalytic efficiency in the mutant aspartate-27→serine *Escherichia coli* dihydrofolate reductase. *Biochemistry* **29**, 8561-8569
10. Li, L. and Benkovic, S.J. (1991) Impact on catalysis of secondary structure manipulation of the $\alpha$ C-helix of *Escherichia coli* dihydrofolate reductase. *Biochemistry* **30**, 1470-1478
11. Sawaya, M.R. and Kraut, J. (1997) Loop and subdomain movements in the mechanism of *Escherichia coli* dihydrofolate reductase: Crystallographic evidence. *Biochemistry* **36**, 586-603
12. Li, L., Falzone, C.J., Wright, P.E., and Benkovic, S.J. (1992) Functional role of a mobile loop of *Escherichia coli* dihydrofolate reductase in transition-state stabilization. *Biochemistry* **32**, 7826-7833
13. Tan, X.H., Huang, S.M., Ratnam, M., Thompson, P.D., and Freisheim, J.H. (1990) The importance of loop region residues 40-46 in human dihydrofolate reductase as revealed by site-directed mutagenesis. *J. Biol. Chem.* **265**, 8027-8032
14. Gekko, K., Yamagami, K., Kunori, Y., Ichihara, S., Kodama, M., and Iwakura, M. (1993) Effects of point mutations in a flexible loop on the stability and enzymatic function of *Escherichia coli* dihydrofolate reductase. *J. Biochem.* **113**, 74-80
15. Gekko, K., Kunori, Y., Takeuchi, H., Ichihara, S., and Kodama, M. (1994) Point mutations at glycine-121 of *Escherichia coli* dihydrofolate reductase: Important roles of a flexible loop in the stability and function. *J. Biochem.* **116**, 34-41
16. Ohmae, E., Iriyama, K., Ichihara, S., and Gekko, K. (1996) Effects of point mutations at the flexible loop glycine-67 of *Escherichia coli* dihydrofolate reductase on its stability and function. *J. Biochem.* **119**, 703-710
17. Gekko, K., Tamura, Y., Ohmae, E., Hayashi, H., Kagamiyama, H., and Ueno, H. (1996) A large compressibility change of protein induced by a single amino acid substitution. *Protein Sci.* **5**, 542-545
18. Epstein, D.M., Benkovic, S.J., and Wright, P.E. (1995) Dynamics of the dihydrofolate reductase-folate complex: catalytic sites and regions known to undergo conformational change exhibit diverse dynamical features. *Biochemistry* **34**, 11037-11048
19. Iwakura, M., Jones, B.E., Luo, J., and Matthews, C.R. (1995) A strategy for testing the suitability of cysteine replacements in dihydrofolate reductase from *Escherichia coli*. *J. Biochem.* **117**, 480-488
20. Vieira, J. and Messing, J. (1987) Production of single-stranded plasmid DNA in *Methods in Enzymology* (Wu, R. and Grossman, L., eds.) Vol. 153, pp. 3-11, Academic Press, New York
21. Nakagawa, T. and Oyanagi, Y. (1980) Program system SALS for nonlinear least-squares fitting in experimental sciences in *Recent Developments in Statistical Inference and Data Analysis* (Matsushita, K., ed.) pp. 221-225, North Holland Publishing Company, Amsterdam
22. Pace, C.N. (1986) Determination and analysis of urea and guanidine hydrochloride denaturation curves in *Methods in Enzymology* (Hirs, C.H.W. and Timasheff, S.N., eds.) Vol. 131, pp. 267-280, Academic Press, New York
23. Williams, J.W., Morrison, J.F., and Duggleby, R.G. (1979) Methotrexate, a high-affinity pseudosubstrate of dihydrofolate reductase. *Biochemistry* **18**, 2567-2573
24. Penner, M.H. and Frieden, C. (1985) Substrate-induced hysteresis in the activity of *Escherichia coli* dihydrofolate reductase. *J. Biol. Chem.* **260**, 5366-5369
25. Stone, S.R. and Morrison, J.F. (1982) Kinetic mechanism of the reaction catalyzed by dihydrofolate reductase from *Escherichia coli*. *Biochemistry* **21**, 3757-3765
26. Touchette, N.A., Perry, K.M., and Matthews, C.R. (1986) Folding of dihydrofolate reductase from *Escherichia coli*. *Biochemistry* **25**, 5445-5452
27. Perry, K.M., Onuffer, J.J., Touchette, N.A., Herndon, C.S., Gittelman, M.S., Matthews, C.R., Chen, J.T., Mayer, R.J., Taira, K., Benkovic, S.J., Howell, E.E., and Kraut, J. (1987) Effect of single amino acid replacements on the folding and stability of dihydrofolate reductase from *Escherichia coli*. *Biochemistry* **26**, 2674-2682
28. Ohmae, E., Iriyama, Y., Ichihara, S., and Gekko, K. (1998) Nonadditive effects of double mutations at the flexible loops, glycine-67 and glycine-121, of *Escherichia coli* dihydrofolate reductase on its stability and function. *J. Biochem.* **123**, 33-41
29. Ahrweiler, P.M. and Frieden, C. (1991) Effects of point mutations in a hinge region on the stability, folding, and enzymatic activity of *Escherichia coli* dihydrofolate reductase. *Biochemistry* **30**, 7801-7809
30. Shortle, D., Stites, W.E., and Meeker, A.K. (1990) Contributions of the large hydrophobic amino acids to the stability of staphylococcal nuclease. *Biochemistry* **29**, 8033-8041
31. Green, S.M., Meeker, A.K., and Shortle, D. (1992) Contributions of the polar, uncharged amino acids to the stability of staphylococcal nuclease: Evidence for mutational effects on the free energy of the denatured state. *Biochemistry* **31**, 5717-5728
32. Takano, K., Ogasahara, K., Kaneda, H., Yamagata, Y., Fujii, S., Kanaya, E., Kikuchi, M., Oobatake, M., and Yutani, K. (1995) Contribution of hydrophobic residues to the stability of human lysozyme: calorimetric studies and X-ray structural analysis of the five isoleucine to valine mutants. *J. Mol. Biol.* **254**, 62-76
33. Takano, K., Yamagata, Y., Fujii, S., and Yutani, K. (1997) Contribution of the hydrophobic effect to the stability of human lysozyme: calorimetric studies and X-ray structural analyses of the nine valine to alanine mutants. *Biochemistry* **36**, 688-698
34. Yutani, K., Ogasahara, K., Tsujita, T., and Sugino, Y. (1987) Dependence of conformational stability on hydrophobicity of the amino acid residue in a series of variant proteins substituted at a unique position of tryptophan synthase $\alpha$ subunit. *Proc. Natl. Acad. Sci. USA* **84**, 4441-4444
35. Matsumura, M., Becktel, W.J., and Matthews, B.W. (1988) Hydrophobic stabilization in T4 lysozyme determined directly by multiple substitutions of Ile 3. *Nature* **334**, 406-410
36. Matsumura, M., Yahanda, S., Yasumura, S., Yutani, K., and Aiba, S. (1988) Role of tyrosine-80 in the stability of kanamycin nucleotidyltransferase analyzed by site-directed mutagenesis. *Eur. J. Biochem.* **171**, 715-720

37. Kellis, J.T., Nyberg, K., and Fersht, A.R. (1989) Energetics of complementary side-chain packing in a protein hydrophobic core. *Biochemistry* **28**, 4914-4922
38. Kauzmann, W. (1959) Some factors in the interpretation of protein denaturation. *Adv. Protein Chem.* **14**, 1-63
39. Lim, W.A., Farruggio, D.C., and Sauer, R.T. (1992) Structural and energetic consequences of disruptive mutations in a protein core. *Biochemistry* **31**, 4324-4333
40. Green, S.M. and Shortle, D. (1993) Patterns of nonadditivity between pairs of stability mutations in staphylococcal nuclease. *Biochemistry* **32**, 10131-10139
41. Pakula, A.A. and Sauer, R.T. (1990) Reverse hydrophobic effects relieved by amino-acid substitutions at a protein surface. *Nature* **344**, 363-364
42. Bowler, B.E., May, K., Zaragoza, T., York, P., Dong, A., and Caughey, W.S. (1993) Destabilizing effects of replacing a surface lysine of cytochrome *c* with aromatic amino acids: Implications for the denatured state. *Biochemistry* **32**, 183-190
43. Nozaki, Y. and Tanford, C. (1971) The solubility of amino acids and two glycine peptides in aqueous ethanol and dioxane solutions. *J. Biol. Chem.* **246**, 2211-2217
44. Matthews, S.J., Jandu, S.K., and Leatherbarrow, R.J. (1993) $^{13}C$ NMR study of the effects of mutation on the tryptophan dynamics in chymotrypsin inhibitor 2: Correlations with structure and stability. *Biochemistry* **32**, 657-662
45. Eriksson, A.E., Baase, W.A., and Matthews, B.W. (1993) Similar hydrophobic replacements of Leu99 and Phe153 within the core of T4 lysozyme have different structural and thermodynamic consequences. *J. Mol. Biol.* **229**, 747-769
46. Gekko, K. and Yamagami, K. (1991) Flexibility of food proteins as revealed by compressibility. *J. Agric. Food Chem.* **39**, 57-62
47. Schellman, J.A. (1978) Solvent denaturation. *Biopolymers* **17**, 1305-1322
48. Pace, C.N., Laurents, D.V., and Thomson, J.A. (1990) pH dependence of the urea and guanidine hydrochloride denaturation of ribonuclease A and ribonuclease T1. *Biochemistry* **29**, 2564-2572
49. Zamyatnin, A.A. (1984) Amino acid, peptide, and protein volume in solution. *Annu. Rev. Biophys. Bioeng.* **13**, 145-165
50. Kraulis, P.J. (1991) MOLSCRIPT: a program to produce both detailed and schematic plots of protein structures. *J. Appl. Crystallogr.* **24**, 946-950